Millennial Variations and a Mid-Holocene Step Change in Northern Mid-latitude Moisture Gradients

Bryan N Shuman (bshuman@uwyo.edu)
University of Wyoming https://orcid.org/0000-0002-8149-8925

Research Article

Keywords: Hydroclimate, lake levels, Holocene, North America, Africa, North Atlantic

Posted Date: February 19th, 2021

DOI: https://doi.org/10.21203/rs.3.rs-238291/v1

Abstract

Holocene records reveal a constantly varying hydroclimate characterized by responses to precession punctuated by decadal-to-centennial ‘megadroughts’ and rapid state shifts. How such changes relate across space and time can reveal the underlying dynamics and how external forcing, intrinsic variability, and various feedbacks interact to alter societally critical water supplies. Here, Holocene water-level changes were examined in two groups of North American lakes to systematically characterize millennial-scale hydroclimate variability and potential large-scale state changes. The records constrain changes at the ends of the large hydroclimate gradient between the semi-arid Rocky Mountains and the humid Atlantic coast. Geophysical surveys and 40 radiocarbon-dated sediment cores provide direct measures of past shoreline positions from the 12 lakes. None exhibited stable Holocene water levels. Together they show a steep east-west gradient from 9-5.5 ka and again from 4.5-2.1 ka. The gradient was unusually weak from 11-9, 5.5-4.5, and after 2.1 ka when Rocky Mountain lakes reached their maxima. Consistent with interconnected atmospheric circulation and land surface energy budget changes, the gradient steepness correlates with mid-continental summer temperature changes (r = 0.73) with a cool, wet mid-continent associated with a weak hydroclimatic gradient, such as during the anomalous mid-Holocene fluctuation from 5.5-4.5 ka. The millennial-scale variability interacted with long-term trends to rapidly increase effective moisture in the west at 5.5 ka, potentially as part of state shifts extending to the Sahel. The interconnected changes underscore the possibility that poorly diagnosed centennial-to-millennial variability could accelerate some Holocene trends to produce abrupt shifts without requiring strong threshold effects.

Introduction

Interglacial temperatures may be broadly stable (Marsicek et al. 2018; Kaufman et al. 2020), but interglacial hydroclimates are not (Cullen et al. 2000; deMenocal et al. 2000a; Cook et al. 2015; Routson et al. 2019; Liefert and Shuman 2020). Geological records of the last ~11,000 years reveal that hydroclimates can change abruptly even when climate forcing is modest. Some Holocene changes in forcing, such as the accelerated reduction in the Laurentide Ice Sheet by ca. 8.2 ka (thousand years before CE 1950)(Barber et al. 1999; Dyke 2004), produced major hydroclimatic changes over large areas (Shuman et al. 2002; Williams et al. 2010; Bhattacharya et al. 2018). Other changes represent more complex, non-linear or stochastic dynamics such as the rapid state changes that affected some regions from the Sahel to central North America at ca. 5.5 ka (deMenocal et al. 2000a; McGee et al. 2013; Shuman and Marsicek 2016) or multi-century events such as those documented in some regions at 4.2 and 2.7 ka (Cullen et al. 2000; Martin-Puertas et al. 2012). The diagnoses of such changes have been debated (Kropelin et al. 2008; Wanner et al. 2011; Shanahan et al. 2015), but they illuminate the risk that unforced changes can arise from ocean-atmosphere dynamics (Shanahan et al. 2009; Shuman et al. 2019) or that thresholds and feedbacks can amplify weak forcing for centuries or longer (Claussen et al. 1999; Renssen et al. 2006; Pausata et al. 2016).

Geological evidence of past lake-level changes represent an archive of Holocene hydroclimate changes that can be systematically evaluated over large areas to investigate such dynamics (Harrison et al. 2015). Across the large precipitation gradient in mid-latitude North America, where annual precipitation falls from >1500 to <700 mm/yr between the Atlantic coast and the Rocky Mountains, many small lakes and ponds responded to Holocene changes (Stone and Fritz 2013; Liefert and Shuman 2020). As they did, lake shorelines changed

position and sediment stratigraphies preserved evidence of these shifts (Winkler et al. 1986; Digerfeldt et al. 1992). Where lakes rose, the area of fine-grained muds deposited beneath deep water expanded. Where lakes fell during dry periods, the area of muds contracted as shoreline sands expanded basinward. The changes appear clearly in geophysical (e.g., ground-penetrating radar) surveys of the lake sediments and can be analyzed and radiocarbon dated when sampled by transects of sediment cores collected in shallow water within tens of meters of the modern shorelines (Digerfeldt 1986; Pribyl and Shuman 2014).

Over the past decade, over a dozen lakes at either end of the mid-latitude moisture gradient across central and eastern North America have been examined using the same systematic approach (Pribyl and Shuman 2014) involving 1) geophysical surveys of dozens of lakes in each region to identify target sites with well-defined sequences of paleoshorelines, 2) collection of transects of sediment cores from different water depths and distances from shore to sample paleoshoreline deposits in each target lake, 3) analyses and radiocarbon dating of the core sedimentology, and 4) systematic reconstruction of lake elevations based on application of a decision-tree algorithm to the core data (Shuman et al. 2009, 2014, 2015; Newby et al. 2011, 2014; Minckley et al. 2012; Marsicek et al. 2013; Pribyl and Shuman 2014; Shuman and Burrell 2017; Shuman and Serravezza 2017). The decision-tree approach creates ensembles of reconstructions for each lake by iteratively classifying sediments within each core as representing shallow or deep environments and then using the classified data from multiple cores to systematically infer the changing elevations of the boundary between the two facies (i.e., the lower elevational limit of shoreline sediments) through time as a measure of lake-level history (Marsicek et al. 2013; Pribyl and Shuman 2014).

In the northeastern United States, closely co-located lakes were studied to replicate the reconstruction results (Newby et al. 2014; Shuman and Burrell 2017), which were found to include replicable patterns of both multi-millennial trends and multi-century variations. The variations correlate with pollen-inferred annual precipitation reconstructions, which accurately drove forward models of transect core stratigraphic features (Shuman et al. 2019). Here, the results are compared to those from lakes in the semi-arid Rocky Mountain region at the opposite end of the moisture gradient, which also reveal a range of Holocene variations including evidence of north-south changes in effective precipitation over centuries to millennia (Shuman et al. 2014; Shuman and Serravezza 2017).

These lake-level reconstructions are synthesized here to constrain the dynamics of the east-west precipitation gradient controlled by delivery of moisture from the Atlantic Ocean. Potential influences include orbital forcing and ocean variability (Webb III et al. 1998; Harrison et al. 2003; Diffenbaugh et al. 2006; Shin et al. 2006; Mantsis et al. 2013) as well as monsoon-related dynamics and surface heating in north Africa (Muschitiello et al. 2015; Kelly et al. 2018; Sun et al. 2019). The lakes only represent two end-member regions, and interpretations are inherently limited as a result, but the comparisons provide evidence of Holocene changes in the continental moisture gradient grounded in direct physical evidence of past water-level changes. A larger network of nearly 200 lakes with some geomorphic or stratigraphic evidence of lake-level change shows substantial long-term hydroclimate changes across North America, but most of the records involved lack detail (Liefert and Shuman 2020). Just as maps and atlases of dendroclimatic drought reconstructions reveal the power of using a single, coherent approach over broad geographic areas to study the synoptic patterns of hydroclimate change at interannual to decadal scales (Cook et al. 1999, 2007, 2015), the comparison of reconstructions derived from 40 radiocarbon-dated sediment cores from 12 lakes clustered in four U.S. states

offer a systematic perspective on the centennial-to-millennial dynamics of a major mid-latitude moisture gradient spanning several thousand kilometers.

Methods

The twelve lake-level reconstructions discussed here cover at least the past 4000 years and ten span the whole Holocene (Table 1). They represent three regions: the northeastern U.S., including coastal (New Long and Deep ponds) and inland areas (Davis and Blanding ponds); the central Rocky Mountains in both northwest (Rainbow Lake and Lake of the Woods) and northcentral Wyoming (Duncan and Lower Paintock lakes); the southern Rocky Mountains along the Colorado-Wyoming border (Little Windy, Upper Big Creek, and Hidden lakes) and central Colorado (Emerald Pond). For simplicity, the groups are referred to below as representing eastern (New Long, Deep, Davis, Blanding) versus western areas (Rainbow, Woods, Duncan, Paintrock, Little Windy, Upper Big Creek, Hidden, Emerald), or when further geographic distinction is needed, the Northeast, northwest (NW) Wyoming, and Colorado.

All of the reconstructions were developed using surveys of paleoshoreline deposits made using ground-penetrating radar (GPR) and derive directly from grain size, loss-on-ignition, or x-ray fluoresce (XRF) data that document facies changes in at least two cores collected at different water depths; all records were interpreted using the same decision-tree approach (Pribyl and Shuman 2014) in R (R Core Development Team 2009). Each represents the median of an ensemble of reconstructions that account for multiple assumptions in the method and the independent chronologies of multiple cores (Marsicek et al. 2013; Pribyl and Shuman 2014). Only changes robust to the reconstruction uncertainty are emphasized. The major changes discussed here appear replicated by near-by lakes. Previous studies have used synchrony analyses based on ensembles of core ages to examine the age uncertainties associated with the millennial-to-centennial changes (Newby et al. 2014; Shuman et al. 2014) and the results summarized here are robust within those uncertainties.

For comparison, all reconstructions have been converted to z-scores by subtracting their mean and normalizing by the standard deviation of the past 8000 years. Principal components analysis (PCA) was conducted to compare the records using functions in base R (R Core Development Team 2009). PCA was conducted using all full Holocene records as well as just those from the western and eastern regions separately.

Results

Declines in the reconstructed water levels indicate changes in the elevational extent of sandy littoral sediments, which interrupted deep-water mud accumulation in near-shore cores from the 12 lakes; reconstructed increases represent periods of shoreward expansion of muds (Fig. 1). The records indicate that all of the lakes experienced multiple millennia when they were lower than today, although the timing varies by region. Additional rapid changes or multi-century variability further distinguish the different regions with added variability among individual lakes resulting from local hydrogeological influences or reconstruction limitations (Fig. 1).

Regional averages affirm patterns common across multiple lakes (Fig. 2). Eastern lakes all indicate significantly lower than modern water levels prior to ca. 8 ka (Fig. 1-2, blue lines), but western lakes indicate maximum lowering both in the late-Pleistocene (>11 ka) and during portions of the mid-Holocene at ca. 8-2 ka (Fig. 1-2, orange and black lines).

3.1 Major millennial-to-centennial features

In eastern lakes, water levels rose rapidly between 10-8 ka with additional increases common afterward, especially in coastal lakes (New Long and Deep ponds). Multiple multi-century fluctuations affected these records since 8 ka with low water phases widely recorded at 4.2-3.9, 2.9-2.1, and 1.3-1.2 ka (late-Holocene gray bars, Fig. 1-2), which are well constrained by multiple ^{14}C ages at multiple sites (Newby et al. 2014; Shuman and Burrell 2017). Inland and coastal areas record contrasting directions of change from ca. 5.5-4.5 ka with inland lakes (Davis and Blanding ponds) falling and coastal lakes (New Long and Deep ponds) rising (gray bar, Fig. 1).

In most western lakes, water levels rose earlier than eastern lakes (Fig. 1-2). Most record late-Pleistocene minima, which specifically date to the Younger Dryas chronozone from ca. 12.6-11.3 ka at Lower Paintrock Lake, Lake of the Woods, and Upper Big Creek Lakes (Fig. 1). Lakes in northwest Wyoming then reached maxima at near-modern levels from ca. 10.5-9.2 ka (gray bar, Fig. 1-2), and Colorado lakes, and the eastern most northern Wyoming lake (Duncan Lake), followed with maxima from ca. 9.2-8.2 ka (orange lines, Fig. 1-2). These lakes then fell with low levels recorded from ca. 8-5.5 ka in northwestern Wyoming (black lines, Fig. 1-2) and from ca. 7-5.5 ka in Colorado (orange lines, Fig. 1-2). Two Colorado lakes (Hidden, Emerald) have no records of early Holocene variations and only the contain stratigraphic evidence of late-Holocene changes (Shuman et al. 2009, 2014).

An increase in water levels at ca. 5.5 ka terminated or interrupted the mid-Holocene low water phase at nearly all western lakes (Fig. 1-2). The rise is not significantly different in time between Lake of the Woods in northern Wyoming and Emerald Lake in central Colorado (Shuman et al. 2014). After the rise, many of the southern lakes fell again and reached second minima before ca. 2.1 ka. Pronounced low water episodes developed by ca. 4 ka at Paintrock, Little Windy, Big Creek, and Emerald lakes (Fig. 1-2). Nearly all lakes have been near their modern high levels for the past two millennia.

3.2 Principal Components Analysis

The first principal component of the lake-level dataset captures 55% of the variance and represents a common long increase in moisture across all sites (top, Fig. 3). The second component, representing 15% of the variance, summarizes the north-south differences between northwest Wyoming (blue symbols, middle map in Fig. 3) and Colorado (orange symbols, middle map in Fig. 3). The second component scores (middle, Fig. 3) capture a set of latitudinal contrasts created when 1) northern lakes declined before southern lakes before ca. 8 ka and 2) the decline of southern lakes from ca. 4.2-2.1 ka when northern lakes began to rise (Fig. 2).

The third component represents major changes in the east-west gradient and 13% of the variance in the dataset (bottom, Fig. 3). The scores emphasize that the moisture contrast between these areas was

- muted in the early Holocene before ca. 9 ka when western lakes were high and eastern lakes low,
- amplified as western lakes fell and eastern lakes rose from ca. 9-5.5 ka,
- relaxed during a millennial anomaly from ca. 5.5-4.5 ka when most western lakes rose and the two eastern inland lakes (Davis and Blanding) fell, and
- amplified again as Colorado lakes fell and eastern lakes continued to rise from ca. 4.5-2 ka (Fig. 1-2).

PCA specific to each region (Fig. 4) reveals similar patterns with the first component of the western and eastern subsets well predicted by combinations of precession trends and the east-west millennial variations. PC1 of both the eastern and western sub-sets of records track the long-term Holocene increase. The difference between the two (DE-W in Fig. 4C) is not significantly different from PC3 of the full dataset (Fig. 3, bottom). Adding the DE-W curve (or PC3 from Fig. 3) to a scaled precession curve (thin “inso” curves in Fig. 4A-B) replicates the major features of the western PC1 scores (r = 0.95) with a prominent step shift at ca. 5.5 ka; subtracting the DE-W curve replicates the eastern PC1 scores (r = 0.95) with a step change at ca. 4.5 ka (Fig. 4).

The trends recorded by PC3 of the whole dataset (Fig. 3), like the DE-W curve (Fig. 4C), correlate with warm-month temperature reconstructions from the mid-continent (r = 0.73)(Fig. 5) and millennial features of a mean temperature reconstruction for all of Europe and North America (r = -0.60)(Marsicek et al. 2018). The mid-continent mean temperature of the warmest month reconstruction based on the average of 6 detailed temperatures records from Rice Lake, ND, to Chatsworth Bog, IL, (thick black line, Fig. 5) is replicated by the individual reconstruction from a seventh centrally located site, Sharkey Lake, MN (thin black line, Fig. 5) (Shuman and Marsicek, 2016). Major features of the east-west difference also correlate with the aeolian dust record from Elk Lake, Minnesota (Dean 1997)(bottom, Fig. 5).

Discussion

The records synthesized here confirm that lakes across mid-latitude North America have fluctuated on a wide range of time scales despite their locations in humid or snow-dominated regions. Their fluctuations indicate multi-millennial to centennial variations in the moisture gradient across semi-arid to humid mid-latitude North America during the Holocene when external climate forcing was modest and monotonic. At face value, they imply three major geographic patterns of hydrologic change during the Holocene (Fig. 3).

First, effective moisture increased over much of the region since the last glacial period. Late-Pleistocene climates may have been arid across much of the region as most lakes in both the eastern and western clusters were low from 15-11 ka (Fig. 1-2). In addition to effects related to the ice sheets, the change may relate to long-term warming driven by greenhouse gas forcing, as well as winter insolation anomalies (Liu et al. 2014; Bova et al. 2021), which could have increased the water vapor available to storms, particularly in winter. Any increase in water vapor was likely then amplified by insolation-driven changes in the tropics-to-polar thermal gradient that favored increased cyclogenesis and therefore production of precipitation from water vapor over the course of the Holocene (Routson et al. 2019).

Second, the east-west gradient has not been stable, but varied in strength on multi-millennial time scales (Fig. 2-3). A rise in the level of western lakes marks the beginning of the Holocene and represents a reduced

gradient before 8 ka compared to today (Fig. 2). Other mid-continental moisture records also provide evidence of high effective moisture in the early Holocene (prior to the mid-Holocene arid period there), such as represented by dust deposition at Elk Lake, Minnesota (Dean 1997)(Fig. 5), diatom records from sites such as Moon Lake, South Dakota (Laird et al. 1996), and numerous fossil pollen records (Bartlein et al. 1984; Bartlein and Whitlock 1993; Grimm 2001; Nelson and Hu 2008; Williams et al. 2010; Grimm et al. 2011).

Rocky Mountain lake levels likely rose at 11 ka in response to changes in moisture delivery caused by the acceleration of Atlantic Meridional Overturning Circulation at the end of the Younger Dryas (McManus et al. 2004; Zhang and Delworth 2005), but the decline in western water-levels by ca. 8 ka coincides with the diminished influence of the Laurentide ice sheet (Fig. 5). Prior to 8 ka, the presence of a large, intact Laurentide Ice Sheet and its associated glacial anti-cyclone reduced the influence of the sub-tropical high and advection of moisture in eastern North America (Shuman et al. 2002), while enhancing moisture delivery to mid-latitude central and western North America (Williams et al. 2010; Oster et al. 2015; Lora et al. 2017; Morrill et al. 2018). The effects would have favored the weak early-Holocene gradient, but after 8 ka, eastern lakes rose, western lakes fell, and the east-west gradient appears to have become steeper than today (Fig. 2).

Subsequent weakening of the gradient re-developed from 5.5-4.5 before it returned to a near modern difference (Fig. 2-4). The weak gradient (wet west-dry east) coincided on millennial time scales with cool mid-continent summers whereas warm continental summers correlated with a strong gradient (dry west-wet east) at other times in the Holocene (Fig. 5). The relationship could relate to reinforcing changes between precipitation, soil moisture, and the resulting effects of latent heating on air temperatures (Oglesby and Erickson 1989; Notaro and Zarrin 2011), but potentially also arose from the overarching atmospheric and ocean circulation changes (O'Brien et al. 1995; Oppo et al. 2003), which could have produced phases of mid-Holocene cooling in central North America (Muschitiello et al. 2015) in conjunction with regional moistening (Kelly et al. 2018).

Third, the latitudinal distribution of moisture along the Rocky Mountains also varied on multi-millennial timescales (Fig. 2-3). Enhanced aridity in the mid-Holocene affected Wyoming from ca. 9-5.5 ka when it extended from the Great Basin to the northern Great Plains (Mock and Brunelle-Daines 1999; Hermann et al. 2018; Liefert and Shuman 2020). Fossil pollen indicate an eastward expansion of prairie in Minnesota (Nelson and Hu 2008) and aeolian datasets indicate increased dune and loess activity in the northern Great Plains (Dean 1997; Miao et al. 2007b)(Fig. 5). Northern Rocky Mountain forest composition during this time also shifted in favor of xeric taxa (Whitlock 1993) and western forest-steppe ecotones shifted as areas of grasslands expanded (Macdonald 1989; Alt et al. 2018).

In Colorado, maximum aridity occurred later from 8-2 ka (Fig. 2-3). The north-south difference in the timing of the Rocky Mountain aridity could represent long-term shifts in winter precipitation patterns similar to those associated with interannual to multidecadal variations over the Pacific Ocean (Wise 2010; Pederson et al. 2011). However, the difference between PC2 and PC3 (Fig. 3) indicates that the western lakes were influenced by multiple dynamics. Both regions experienced at least a modest reduction in the aridity at ca. 5.5-4.5 ka, although the wet millennial period appears to have been drier than today in the south (e.g., Upper Big Creek and Emerald lakes).

The increase in western water levels at ca. 5.5 ka may relate to large-scale hemispheric phenomena (Fig. 6-7), connecting African and North American changes in a manner consistent with simulations (Muschitiello et al. 2015; Kelly et al. 2018; Sun et al. 2019). The change coincided with an apparent shift in European and North American mean temperatures and in sea-surface temperatures in the western North Atlantic (Fig. 6)(Kim et al. 2007; Sachs 2007; Marsicek et al. 2018). The change also correlates with other evidence of a non-linear transition in the mid-Holocene over portions of the North Atlantic from Iceland (Larsen et al. 2012).

“Green Sahara” simulations show that the synoptic consequences of a rapid end to the African humid period in the mid-Holocene could have propagated northward to the Arctic via the weakened northern mid-latitude westerlies (Muschitiello et al. 2015; Kelly et al. 2018)(Fig. 7). As anticipated by simulations (Hopcroft and Valdes 2019), dust deposition downwind of the Great Plains declined rapidly as it increased off the coast of west Africa (Fig. 6)(Bradbury and Dean 1993; Dean 1997; deMenocal et al. 2000a; McGee et al. 2013). The changes in the dust loading may be a critical feedback (Pausata et al. 2016; Messori et al. 2019) when foraminifera assemblages in the upwelling region off west Africa also shifted abruptly, consistent with a change in the African monsoon (deMenocal et al. 2000b), which would have provided the thermodynamic mechanism for displacing atmospheric circulation over the Atlantic sub-tropics and enhancing moisture delivery to North America (Kelly et al. 2018).

Consistent with such dynamics, the belt of sub-tropical moisture over west Africa shifted southward at ca. 5.5 ka, rapidly increasing effective moisture in a step-wise reversal of precession-forced drying trends in Ghana (Shanahan et al. 2015) while rapidly accelerating them elsewhere in north Africa (deMenocal and Tierney 2012; Tierney and deMenocal 2013). Abrupt cooling in the Atlantic may have favored the southward shift (Fig. 6)(Kim et al. 2007; Sachs 2007), although it may have coincided with a net warming of adjacent continents (Fig. 6)(Marsicek et al. 2018). Even though the African changes have important spatial differences (Claussen et al. 2017), the rapid increase in effective precipitation at Lake Bosumtwi, Ghana from 5.8-5.2 ka (Shanahan et al. 2015) is synchronous with the rapid drying in the Sahel indicated by increasing dust deposition off west Africa at 5.6-5.1 ka in ODP core 658c (Fig. 8)(deMenocal et al. 2000a). Drying in portions of the Sahel (but not synchronously across the Sahara; Kropelin et al. 2008) parallels modern precipitation correlations associated with shifts in Atlantic pressure fields that increase in precipitation elsewhere, including the Rocky Mountains (Fig. 7A)(Landsea and Gray 1992; Zhang and Delworth 2006; Wang et al. 2012).

The Rocky Mountains have some of the highest correlations with Sahelian precipitation outside of Africa, especially in the northern hemisphere summer months (Fig. 7A). Reduced precipitation in the Sahel tends to coincide with increased African surface pressures and increased 500 mb geopotential heights (Fig. 7B) just as expected in response to a reduction in the African monsoon in response to precessional forcing (Claussen et al. 2017; Kelly et al. 2018). Easterly (dust laden) winds from the Sahel are then enhanced, while mid-latitude westerly zonal velocities decline between central North America and western Europe (Fig. 7C). Specific humidity increases over the Americas (Fig. 7D) as water vapor is advected northward into (Fig. 7F) and not eastward away from (Fig. 7C) the North American mid-continent where uplift produces precipitation (Fig. 7E). The changes in surface heating in Africa, thus, propagate to North America through dynamics linked to the North Atlantic Subtropical High, which have consequences for the east-west moisture gradient and have analogs in mid-Holocene simulations (Kelly et al. 2018).

If the change at 5.5 ka represents a step-shift in Holocene climates that connected Africa, the North Atlantic, and North America (Fig. 6)(deMenocal et al. 2000a; Marsicek et al. 2018), it also marks the beginning of the anomalous millennium when the east-west moisture gradient was reduced (Fig. 3-4). The period from 5.5-4.5 ka appears as a prominent millennial anomaly in many regions of mid-latitude North America (Fig. 5) (Shuman, submitted) and more broadly in the northern hemisphere (Magny and Haas 2004; Mayewski et al. 2004; Marsicek et al. 2018; Helama et al. 2021). At the time, inland lakes (Blanding, Davis) in the northeast were low, but coastal lakes (Deep, New Long) rose (Fig. 1)(Newby et al. 2014; Shuman and Burrell 2017). In the Great Plains, loess activity declined at 5.5-5.2 ka, remained low for >300 years, and then increased after 4.9-4.5 ka (Fig. 6)(Dean 1997). A prominent A_b soil horizon amid the Holocene Bignell Loess in the western Great Plains dates to the same wet millennial period (Miao et al. 2007a) when prairie pollen records mark a millennial decline in *Ambrosia* (ragweed) pollen (Grimm 2001) and diatoms indicate a millennial freshening of Moon Lake, North Dakota (Laird et al. 1996). Further west, submerged tree stumps in Lake Tahoe, California, document aridity and low water from 5.75-4.44 ka (Lindstrom 1990; Benson et al. 2002). Similar mid-Holocene millennial anomalies exist in Africa (Thompson et al. 2002; Berke et al. 2012).

Potentially, as indicated by combinations of precessional trends and the millennial east-west changes (Fig. 4), the apparent step change at 5.5 ka could represent the interference of long-term Holocene trends and a prominent millennial-scale variation (Fig. 8). In some areas, such as in the northern Rocky Mountains (Fig. 4B) and the Sahel as recorded by ODP658c (Fig. 8A-B), the two changes constructively interfere to accelerate long-term trends, but in other areas, such as Elk Lake, Minnesota (Fig. 5) and Lake Bosumtwi, Ghana (Fig. 8A), the two patterns may have negatively interfered to produce a millennial oscillation (Fig. 5). The outcome depends upon the relative magnitudes and signs of the trends and millennial fluctuation, such that negative interference could appear as a delayed abrupt shift like recorded at ca. 4.5 ka in northeastern lakes (Fig. 4A), in eastern North American speleothems (Hardt et al. 2010), or potentially in southern hemisphere regions with opposing insolation trends (Cruz et al. 2009). The timing can also depend on interactions with other patterns of variability such as reconstructed over the northwest Atlantic and observed in the northeastern coastal lakes (Fig. 1)(Shuman, submitted; Shuman et al. 2019).

Whether the two phenomena (step change and millennial oscillation) are linked is important because a step-shift spanning from Africa to North America could relate to threshold effects related to surface-atmosphere or dust feedbacks (Claussen et al. 1999; Pausata et al. 2016), but such feedbacks are unlikely to have produced (although they could amplify) a millennial-scale climatic fluctuation. Anomalous conditions from ca. 5.5-4.5 ka could relate to either external volcanic or solar forcing (Hernández et al. 2020; Helama et al. 2021) or internal variability, such as in the North Atlantic (Oppo et al. 2003; Thornalley et al. 2009). The interference with orbital and ice volume trends differs, however, from that observed during abrupt Pleistocene events associated with North Atlantic overturning such as the Younger Dryas (YD) because the east-west gradient in North America decreased after the YD and increased after the anomalous millennium from 5.5-4.5 ka (Fig. 8C). In Africa, Ghana and the Sahel appear to have changed in concert during the YD, but in opposition at 5.5 ka (Fig. 8A).

Conclusions

A network of systematically generated lake-level reconstructions based on 40 radiocarbon-dated sediment cores from the 12 lakes in two regions of North America indicate that the prominent mid-latitude moisture gradient there changed on millennial time scale throughout the Holocene. The changes left direct stratigraphic evidence of hydrologic change, which deserve further investigation, particularly if they demonstrate that climate changes and surface-atmosphere feedbacks in one continent (Muschitiello et al. 2015; Claussen et al. 2017; Kelly et al. 2018) had profound influences on the hydroclimate, ecology, and related human history in another (Kelly et al. 2013; Marsicek et al. 2013). The North American lake-level records raise the possibility, however, that a widespread state change in Holocene climates at ca. 5.5 ka (deMenocal and Tierney 2012; Marsicek et al. 2018) represented the interference of orbitally-paced and millennial variability rather than threshold effects. In either case, North American hydroclimates likely varied on both time scales as part of large-scale dynamics. Different regions experienced differing directions of change becausee of the combinations of multiple mechanisms including Holocene-scale increases in moisture availability, north-south shifts in Rocky Mountain precipitation, and east-west shifts involving the North Atlantic Subtropical High and the Atlantic-African sub-tropics. The variations underscore the risk that critical water resources can experience variations persisting longer than multi-decadal megadroughts, which have yet to be diagnosed and understood dynamically.

Declarations

Acknowledgements

This work was supported by funding from U.S. National Science Foundation (DEB-1856047; EAR-1903729). C. Routson, C. Morrill, and D. Groff kindly provided thoughtful comments on the manuscript.

References

1. Alt M, McWethy DB, Everett R, Whitlock C (2018) Millennial scale climate-fire-vegetation interactions in a mid-elevation mixed coniferous forest, Mission Range, northwestern Montana, USA. Quat Res 90:66–82. https://doi.org/10.1017/qua.2018.25
2. Barber DC, Dyke A, Hillaire-Marcel C, et al (1999) Forcing of the cold event of 8,200 years ago by catastrophic drainage of Laurentide lakes. Nature 400:344–348
3. Bartlein P, Whitlock C (1993) Paleoclimatic interpretation of the Elk Lake pollen record. In: Bradbury JP, Dean W (eds) Elk Lake, Minnesota: Evidence for Rapid Climate Change in the North Central United States (Special Paper 276). Geological Society of America, pp 275–293
4. Bartlein PJ, Fleri EC, Webb T (1984) Holocene climatic change in the northern Midwest: pollen derived estimates. Quat Res 22:361–374
5. Benson L, Kashgarian M, Rye R, et al (2002) Holocene multidecadal and multicentennial droughts affecting Northern California and Nevada. Quat Sci Rev 21:659–682
6. Berger A, Loutre MF (1991) Insolation values for the climate of the last 10 million years. Quat Sci Rev 10:297
7. Berke MA, Johnson TC, Werne JP, et al (2012) A mid-Holocene thermal maximum at the end of the African Humid Period. Earth Planet Sci Lett 351–352:95–104. https://doi.org/10.1016/j.epsl.2012.07.008

8. Bhattacharya T, Tierney JE, Addison JA, Murray JW (2018) Ice-sheet modulation of deglacial North American monsoon intensification. Nat Geosci 11:848–852. https://doi.org/10.1038/s41561-018-0220-7
9. Bova S, Rosenthal Y, Liu Z, et al (2021) Seasonal origin of the thermal maxima at the Holocene and the last interglacial. Nature 589:548–553. https://doi.org/10.1038/s41586-020-03155-x
10. Bradbury JP, Dean WE (1993) Elk Lake, Minnesota: Evidence for Rapid Climate Change in the North Central United States. Geological Society of America, Denver
11. Claussen M, Dallmeyer A, Bader J (2017) Theory and Modeling of the African Humid Period and the Green Sahara. In: Oxf. Res. Encycl. Clim. Sci. https://oxfordre.com/climatescience/view/10.1093/acrefore/9780190228620.001.0001/acrefore-9780190228620-e-532. Accessed 24 Jan 2021
12. Claussen M, Kubatzki C, Brovkin V, et al (1999) Simulation of an abrupt change in Saharan vegetation in the mid-Holocene. Geophys Res Lett 26:2037–2040
13. Cook ER, Meko DM, Stahle DW, Cleaveland MK (1999) Drought reconstructions for the continental United States. J Clim 12:1145–1162
14. Cook ER, Seager R, Cane MA, Stahle DW (2007) North American drought: Reconstructions, causes, and consequences. Earth-Sci Rev 81:93–134
15. Cook ER, Seager R, Kushnir Y, et al (2015) Old World megadroughts and pluvials during the Common Era. Sci Adv 1:e1500561. https://doi.org/10.1126/sciadv.1500561
16. Cruz FW, Vuille M, Burns SJ, et al (2009) Orbitally driven east-west antiphasing of South American precipitation. Nat Geosci 2:210–214
17. Cullen HM, deMenocal PB, Hemming S, et al (2000) Climate change and the collapse of the Akkadian empire: Evidence from the deep sea. Geology 28:379–382. https://doi.org/10.1130/0091-7613(2000)28<379:ccatco>2.0.co;2
18. Dean WE (1997) Rates, timing, and cyclicity of Holocene eolian activity in north-central United States; evidence from varved lake sediments. Geology 25:331–334
19. deMenocal P, Ortiz J, Guilderson T, et al (2000a) Abrupt onset and termination of the African Humid Period:: rapid climate responses to gradual insolation forcing. Quat Sci Rev 19:347–361
20. deMenocal P, Ortiz J, Guilderson T, Sarnthein M (2000b) Coherent High- and Low-Latitude Climate Variability During the Holocene Warm Period. Science 288:2198–2202. https://doi.org/10.1126/science.288.5474.2198
21. deMenocal PB, Tierney JE (2012) Green Sahara: African Humid Periods Paced by Earth's Orbital Changes. Nat Educ Knowl 3:12
22. Diffenbaugh NS, Ashfaq M, Shuman B, et al (2006) Summer aridity in the United States: Response to mid-Holocene changes in insolation and sea surface temperature. Geophys Res Lett 33:L22712
23. Digerfeldt G (1986) Studies on past lake-level fluctuations. In: Berglund BE (ed) Handbook of Holocene Palaeoecology and Palaeohydrology. John Wiley and Sons, Chichester, U. K., pp 127-142.
24. Digerfeldt G, Almendinger JE, Bjorck S (1992) Reconstruction of past lake levels and their relation to groundwater hydrology in the Parkers Prairie sandplain, west-central Minnesota. Palaeoceanography Palaeoclimatol Palaeoecol 94:99

25. Dyke AS (2004) An outline of North American deglaciation with emphasis on central and northern Canada. In: Ehlers J, Gibbard PL (eds) Developments in Quaternary Science. Elsevier, pp 373–424
26. Grimm EC (2001) Trends and palaeoecological problems in the vegetation and climate history of the northern Great Plains, U.S.A. Biol Environ Proc R Ir Acad 99B:1–18
27. Grimm EC, Donovan JJ, Brown KJ (2011) A high-resolution record of climate variability and landscape response from Kettle Lake, northern Great Plains, North America. Quat Sci Rev 30:2626–2650
28. Hardt B, Rowe HD, Springer GS, et al (2010) The seasonality of east central North American precipitation based on three coeval Holocene speleothems from southern West Virginia. Earth Planet Sci Lett 295:342–348
29. Harrison SP, Bartlein PJ, Izumi K, et al (2015) Evaluation of CMIP5 palaeo-simulations to improve climate projections. Nat Clim Change 5:735–743. https://doi.org/10.1038/nclimate2649
30. Harrison SP, Kutzbach JE, Liu Z, et al (2003) Mid-Holocene climates of the Americas: a dynamical response to changed seasonality. Clim Dyn 20:663–688
31. Helama S, Stoffel M, Hall RJ, et al (2021) Recurrent transitions to Little Ice Age-like climatic regimes over the Holocene. Clim Dyn. https://doi.org/10.1007/s00382-021-05669-0
32. Hermann NW, Oster JL, Ibarra DE (2018) Spatial patterns and driving mechanisms of mid-Holocene hydroclimate in western North America. J Quat Sci 33:421–434. https://doi.org/10.1002/jqs.3023
33. Hernández A, Martin-Puertas C, Moffa-Sánchez P, et al (2020) Modes of climate variability: Synthesis and review of proxy-based reconstructions through the Holocene. Earth-Sci Rev 209:103286. https://doi.org/10.1016/j.earscirev.2020.103286
34. Hopcroft PO, Valdes PJ (2019) On the Role of Dust-Climate Feedbacks During the Mid-Holocene. Geophys Res Lett 46:1612–1621. https://doi.org/10.1029/2018GL080483
35. Kaufman D, McKay N, Routson C, et al (2020) A global database of Holocene paleotemperature records. Sci Data 7:115. https://doi.org/10.1038/s41597-020-0445-3
36. Kelly P, Kravitz B, Lu J, Leung LR (2018) Remote Drying in the North Atlantic as a Common Response to Precessional Changes and CO2 Increase Over Land. Geophys Res Lett 45:3615–3624. https://doi.org/10.1002/2017GL076669
37. Kelly RL, Surovell TA, Shuman B, Smith GM (2013) A Continuous Climatic Impact on Holocene Human Population in the Rocky Mountains. Proc Natl Acad Sci 110:443–447. https://doi.org/10.1073/pnas.1201341110
38. Kim J, Meggers H, Rimbu N, et al (2007) Impacts of the North Atlantic gyre circulation on Holocene climate off northwest Africa. Geology 35:387–390. http://dx.doi.org.libproxy.uwyo.edu/10.1605/01.301-0001952419.2007
39. Kropelin S, Verschuren D, Lezine AM, et al (2008) Climate-Driven Ecosystem Succession in the Sahara: The Past 6000 Years. Science 320:765–768. https://doi.org/10.1126/science.1154913
40. Laird KR, Fritz SC, Grimm EC, Mueller PG (1996) Century-scale paleoclimatic reconstruction from Moon Lake, a closed-basin lake in the northern Great Plains. Limnol Oceanogr 41:890–902
41. Landsea CW, Gray WM (1992) The Strong Association between Western Sahelian Monsoon Rainfall and Intense Atlantic Hurricanes. J Clim 5:435–453. https://doi.org/10.1175/1520-

0442(1992)005<0435:tsabws>2.0.co;2

42. Larsen DJ, Miller GH, Geirsdóttir Á, Ólafsdóttir S (2012) Non-linear Holocene climate evolution in the North Atlantic: a high-resolution, multi-proxy record of glacier activity and environmental change from Hvítárvatn, central Iceland. Quat Sci Rev 39:14–25. https://doi.org/10.1016/j.quascirev.2012.02.006
43. Liefert DT, Shuman BN (2020) Pervasive Desiccation of North American Lakes During the Late Quaternary. Geophys Res Lett 47:e2019GL086412. https://doi.org/10.1029/2019GL086412
44. Lindstrom S (1990) Submerged tree stumps as indicators of mid-Holocene aridity in the Lake Tahoe Basin. J Calif Gt Basin Anthropol 12:146–157
45. Liu Z, Zhu J, Rosenthal Y, et al (2014) The Holocene temperature conundrum. Proc Natl Acad Sci 111:E3501–E3505. https://doi.org/10.1073/pnas.1407229111
46. Lora JM, Mitchell JL, Risi C, Tripati AE (2017) North Pacific atmospheric rivers and their influence on western North America at the Last Glacial Maximum. Geophys Res Lett 44:1051–1059. https://doi.org/10.1002/2016GL071541
47. Macdonald GM (1989) Postglacial palaeoecology of the subalpine forest – grassland ecotone of southwestern Alberta: New insights on vegetation and climate change in the Canadian rocky mountains and adjacent foothills. Palaeogeogr Palaeoclimatol Palaeoecol 73:155–173
48. Magny M, Haas JN (2004) A major widespread climatic change around 5300 cal. yr BP at the time of the Alpine Iceman. J Quat Sci 19:423–430. https://doi.org/10.1002/jqs.850
49. Mantsis DF, Clement AC, Kirtman B, et al (2013) Precessional Cycles and Their Influence on the North Pacific and North Atlantic Summer Anticyclones. J Clim 26:4596–4611. https://doi.org/10.1175/JCLI-D-12-00343.1
50. Marsicek J, Shuman BN, Bartlein PJ, et al (2018) Reconciling divergent trends and millennial variations in Holocene temperatures. Nature 554:92–96. https://doi.org/10.1038/nature25464
51. Marsicek JP, Shuman B, Brewer S, et al (2013) Moisture and temperature changes associated with the mid-Holocene Tsuga decline in the northeastern United States. Quat Sci Rev 80:333–342. https://doi.org/10.1016/j.quascirev.2013.09.001
52. Martin-Puertas C, Matthes K, Brauer A, et al (2012) Regional atmospheric circulation shifts induced by a grand solar minimum. Nat Geosci 5:397–401. https://doi.org/10.1038/ngeo1460
53. Mayewski PA, Rohling E, Stager C, et al (2004) Holocene climate variability. Quat Res 62:243
54. McGee D, deMenocal PB, Winckler G, et al (2013) The magnitude, timing and abruptness of changes in North African dust deposition over the last 20,000 yr. Earth Planet Sci Lett 371–372:163–176. https://doi.org/10.1016/j.epsl.2013.03.054
55. McManus JF, Francois R, Gherardi JM, et al (2004) Collapse and rapid resumption of Atlantic meridional circulation linked to deglacial climate changes. Nature 428:834–837
56. Messori G, Gaetani M, Zhang Q, et al (2019) The water cycle of the mid-Holocene West African monsoon: The role of vegetation and dust emission changes. Int J Climatol 39:1927–1939. https://doi.org/10.1002/joc.5924
57. Miao X, Mason JA, Johnson WC, Wang H (2007a) High-resolution proxy record of Holocene climate from a loess section in Southwestern Nebraska, USA. Palaeogeogr Palaeoclimatol Palaeoecol 245:368–381.

https://doi.org/10.1016/j.palaeo.2006.09.004
58. Miao X, Mason JA, Swinehart JB, et al (2007b) A 10,000 year record of dune activity, dust storms, and severe drought in the central Great Plains. Geology 35:119–122
59. Minckley T, Shriver RK, Shuman B (2012) Resilience and regime change in a southern Rocky Mountain ecosystem during the past 17000 years. Ecol Monogr 82:49–68. https://doi.org/10.1890/11-0283.1
60. Mock CJ, Brunelle-Daines AR (1999) A modern analogue of western United States summer palaeoclimate at 6000 years before present. The Holocene 9:541
61. Morrill C, Lowry DP, Hoell A (2018) Thermodynamic and Dynamic Causes of Pluvial Conditions During the Last Glacial Maximum in Western North America. Geophys Res Lett 45:335–345. https://doi.org/10.1002/2017GL075807
62. Muschitiello F, Zhang Q, Sundqvist HS, et al (2015) Arctic climate response to the termination of the African Humid Period. Quat Sci Rev 125:91–97. https://doi.org/10.1016/j.quascirev.2015.08.012
63. Nelson DM, Hu FS (2008) Patterns and drivers of Holocene vegetational change near the prairie-forest ecotone in Minnesota: revisiting McAndrews' transect. New Phytol 179:449–459
64. Newby P, Shuman B, Donnelly JP, et al (2014) Centennial-to-Millennial Hydrologic Trends and Variability along the North Atlantic Coast, U.S.A., during the Holocene. Geophys Res Lett 41:. https://doi.org/10.1002/2014GL060183
65. Newby PE, Shuman BN, Donnelly JP, MacDonald D (2011) Repeated century-scale droughts over the past 13,000 yrs near the Hudson River watershed, USA. Quat Res 75:523–530
66. Notaro M, Zarrin A (2011) Sensitivity of the North American monsoon to antecedent Rocky Mountain snowpack. Geophys Res Lett 38:. https://doi.org/10.1029/2011GL048803
67. O'Brien SR, Mayewski P, Meeker LD, et al (1995) Complexity of Holocene climate as reconstructed from a Greenland ice core. Science 270:1962
68. Oglesby RJ, Erickson DJ (1989) Soil Moisture and the Persistence of North American Drought. J Clim 2:1362–1380
69. Oppo DW, McManus JF, Cullen JL (2003) Palaeo-oceanography: Deepwater variability in the Holocene epoch. Nature 422:277–277
70. Oster JL, Ibarra DE, Winnick MJ, Maher K (2015) Steering of westerly storms over western North America at the Last Glacial Maximum. Nat Geosci 8:201–205. https://doi.org/10.1038/ngeo2365
71. Pausata FSR, Messori G, Zhang Q (2016) Impacts of dust reduction on the northward expansion of the African monsoon during the Green Sahara period. Earth Planet Sci Lett 434:298–307. https://doi.org/10.1016/j.epsl.2015.11.049
72. Pederson GT, Gray ST, Woodhouse CA, et al (2011) The Unusual Nature of Recent Snowpack Declines in the North American Cordillera. Science. https://doi.org/10.1126/science.1201570
73. Pribyl P, Shuman BN (2014) A computational approach to Quaternary lake-level reconstruction applied in the central Rocky Mountains, Wyoming, USA. Quat Res 82:249–259. https://doi.org/10.1016/j.yqres.2014.01.012
74. R Core Development Team (2009) R: A language and environment for statistical computing. R Foundation for Statistical Computing, Vienna, Austria

75. Renssen H, Goosse H, Muscheler R (2006) Coupled climate model simulation of Holocene cooling events: oceanic feedback amplifies solar forcing. Clim Past 2:79–90
76. Routson CC, McKay NP, Kaufman DS, et al (2019) Mid-latitude net precipitation decreased with Arctic warming during the Holocene. Nature 568:83–87. https://doi.org/10.1038/s41586-019-1060-3
77. Sachs JP (2007) Cooling of Northwest Atlantic slope waters during the Holocene. Geophys Res Lett 34:L03609. https://doi.org/10.1029/2006gl028495
78. Shanahan TM, McKay NP, Hughen KA, et al (2015) The time-transgressive termination of the African Humid Period. Nat Geosci 8:140–144. https://doi.org/10.1038/ngeo2329
79. Shanahan TM, Overpeck JT, Anchukaitis KJ, et al (2009) Atlantic Forcing of Persistent Drought in West Africa. Science 324:377–380. https://doi.org/10.1126/science.1166352
80. Shin S-I, Sardeshmukh PD, Webb RS, et al (2006) Understanding the Mid-Holocene Climate. J Clim 19:2801–2817
81. Shuman BN (2021, submitted) Centennial-to-Millennial Holocene Temperature and Hydroclimate Variation in the Northern Mid-Latitudes. Earth Planet Sci Lett, submitted.
82. Shuman B, Bartlein P, Logar N, et al (2002) Parallel climate and vegetation responses to the early-Holocene collapse of the Laurentide Ice Sheet. Quat Sci Rev 21:1793–1805
83. Shuman BN, Burrell SA (2017) Centennial to millennial hydroclimatic fluctuations in the humid northeast United States during the Holocene. Quat Res 1–11. https://doi.org/10.1017/qua.2017.62
84. Shuman BN, Carter GE, Hougardy DD, et al (2014) A north–south moisture dipole at multi-century scales in the Central and Southern Rocky Mountains, U.S.A., during the late Holocene. Rocky Mt Geol 49:33–49. https://doi.org/10.2113/gsrocky.49.1.33
85. Shuman BN, Henderson AK, Colman SM, et al (2009) Holocene Lake-Level Trends in the Rocky Mountains, U.S.A. Quat Sci Rev 28:1861–1879
86. Shuman BN, Marsicek J, Oswald WW, Foster DR (2019) Predictable hydrological and ecological responses to Holocene North Atlantic variability. Proc Natl Acad Sci 116:5985–5990. https://doi.org/10.1073/pnas.1814307116
87. Shuman BN, Marsicek JP (2016) The Structure of Holocene Climate Change in Mid-Latitude North America. Quat Sci Rev 141:38–51
88. Shuman BN, Pribyl P, Buettner J (2015) Hydrologic changes in Colorado during the mid-Holocene and Younger Dryas. Quat Res 84:187–199. https://doi.org/10.1016/j.yqres.2015.07.004
89. Shuman BN, Serravezza M (2017) Patterns of hydroclimatic change in the Rocky Mountains and surrounding regions since the last glacial maximum. Quat Sci Rev 173:58–77. https://doi.org/10.1016/j.quascirev.2017.08.012
90. Stone JR, Fritz SC (2013) LAKE LEVEL STUDIES | North America. In: Elias SA, Mock CJ (eds) Encyclopedia of Quaternary Science (Second Edition). Elsevier, Amsterdam, pp 537–548
91. Sun W, Wang B, Zhang Q, et al (2019) Northern Hemisphere Land Monsoon Precipitation Increased by the Green Sahara During Middle Holocene. Geophys Res Lett 46:9870–9879. https://doi.org/10.1029/2019GL082116

92. Thompson LG, Mosley-Thompson E, Davis ME, et al (2002) Kilimanjaro Ice Core Records: Evidence of Holocene Climate Change in Tropical Africa. Science 298:589–593. https://doi.org/10.1126/science.1073198
93. Thornalley DJR, Elderfield H, McCave IN (2009) Holocene oscillations in temperature and salinity of the surface subpolar North Atlantic. Nature 457:711–714
94. Tierney JE, deMenocal PB (2013) Abrupt Shifts in Horn of Africa Hydroclimate Since the Last Glacial Maximum. Science 342:843–846. https://doi.org/10.1126/science.1240411
95. Wang C, Dong S, Evan AT, et al (2012) Multidecadal Covariability of North Atlantic Sea Surface Temperature, African Dust, Sahel Rainfall, and Atlantic Hurricanes. J Clim 25:5404–5415. https://doi.org/10.1175/jcli-d-11-00413.1
96. Wanner H, Solomina O, Grosjean M, et al (2011) Structure and origin of Holocene cold events. Quat Sci Rev 30:3109–3123. https://doi.org/10.1016/j.quascirev.2011.07.010
97. Webb III T, Anderson KH, Bartlein PJ, Webb RS (1998) Late Quaternary climate change in eastern North America: a comparison of pollen-derived estimates with climate model results. Quat Sci Rev 17:587–606
98. Whitlock C (1993) Postglacial vegetation and climate of Grand-Teton and southern Yellowstone National Parks. Ecol Monogr 63:173–198
99. Williams JW, Shuman B, Bartlein PJ, et al (2010) Rapid, time-transgressive, and variable responses to early Holocene midcontinental drying in North America. Geology 38:135–138. https://doi.org/10.1130/g30413.1
100. Winkler MG, Swain AM, Kutzbach JE (1986) Middle Holocene dry period in the northern midwestern United States: lake levels and pollen stratigraphy. Quat Res 25:235–250
101. Wise EK (2010) Spatiotemporal variability of the precipitation dipole transition zone in the western United States. Geophys Res Lett 37:L07706. https://doi.org/10.1029/2009gl042193
102. Zhang R, Delworth TL (2005) Simulated Tropical Response to a Substantial Weakening of the Atlantic Thermohaline Circulation. J Clim 18:1853–1860
103. Zhang R, Delworth TL (2006) Impact of Atlantic multidecadal oscillations on India/Sahel rainfall and Atlantic hurricanes. Geophys Res Lett 33:L17712. https://doi.org/10.1029/2006gl026267

Tables

Table 1. Lake locations, age control, and principle component (PC) loadings

Number	Site	State	Latitude	Longitude	14C dates	PC1	PC2	PC3	Citation for reconstruction
1	New Long Pond	MA	41.85	-70.68	52	**-0.36**	0.09	**0.36**	Newby et al. (2009; 2014)
2	Deep Pond	MA	41.56	-70.64	53	**-0.4**	-0.16	0.15	Marsicek et al. (2013)
3	Davis Pond	MA	42.14	-73.41	31	**-0.4**	0	0.18	Newby et al. (2011; 2014)
4	Blanding Lake	PA	41.79	-75.68	24	**-0.34**	0.22	0.22	Shuman and Burrell (2017)
5	Rainbow Lake	WY	44.94	-109.50	29	-0.29	**-0.44**	**-0.35**	Shuman and Serravezza (2017)
6	Lake of the Woods	WY	43.48	-109.89	21	-0.23	**-0.31**	**-0.54**	Pribyl and Shuman (2014)
7	Duncan Lake	WY	44.65	-107.45	25	**-0.39**	0.07	-0.16	Shuman and Serravezza (2017)
9	Lower Paintrock Lake	WY	44.39	-107.38	39	**-0.3**	0.08	0.22	Rust and Minckley (2019)
8	Little Windy Hill Pond	WY	41.43	-106.33	18	-0.24	**0.38**	**-0.42**	Minckley et al. (2012)
10	Upper Big Creek Lake	CO	40.91	-106.62	7	-0.02	**0.68**	**-0.33**	Shuman et al. (2015)
11	Hidden Lake	CO	40.51	-106.61	16				Shuman et al. (2009)
12	Emerald Lake	CO	39.15	-106.41	29				Shuman et al. (2014)

Figures

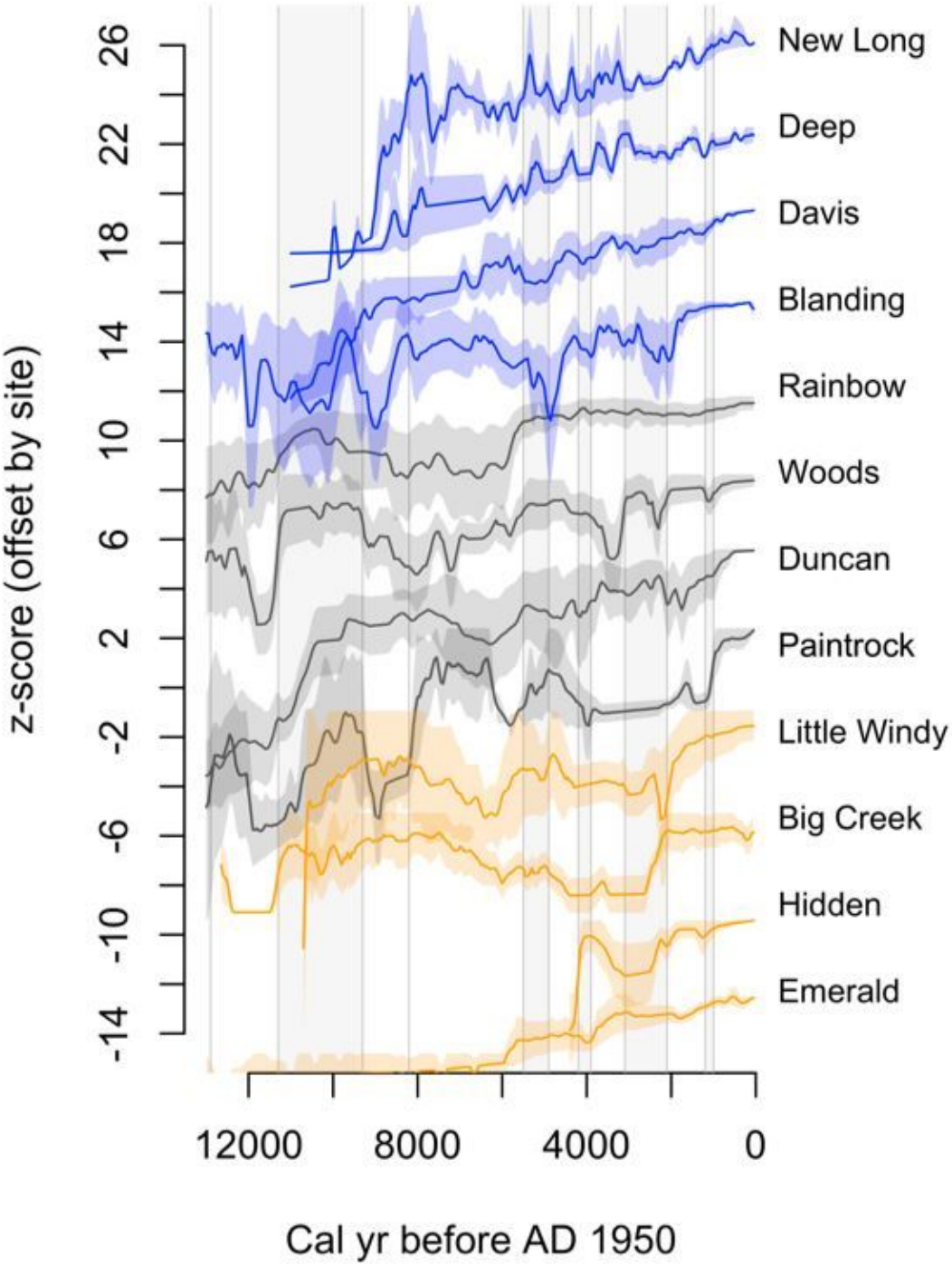

Figure 1

Twelve quantified lake-level reconstructions spanning since at least 4 ka from three regions: the Northeast (blue), NW Wyoming (black), and Colorado (orange). The records are plotted as z-scores (departures from the mean of each record measured in numbers of standard deviations) and are offset for clarity. Gray bars highlight intervals of interest in at least one region: well-dated late-Holocene events in the Northeast (Newby et al. 2014) and an early-Holocene dry period in the east coincident with a wet period in Wyoming at ca. 11.3-9.2 ka (Shuman and Serravezza 2017). Gray lines indicate 12.7 and 8.2 ka.

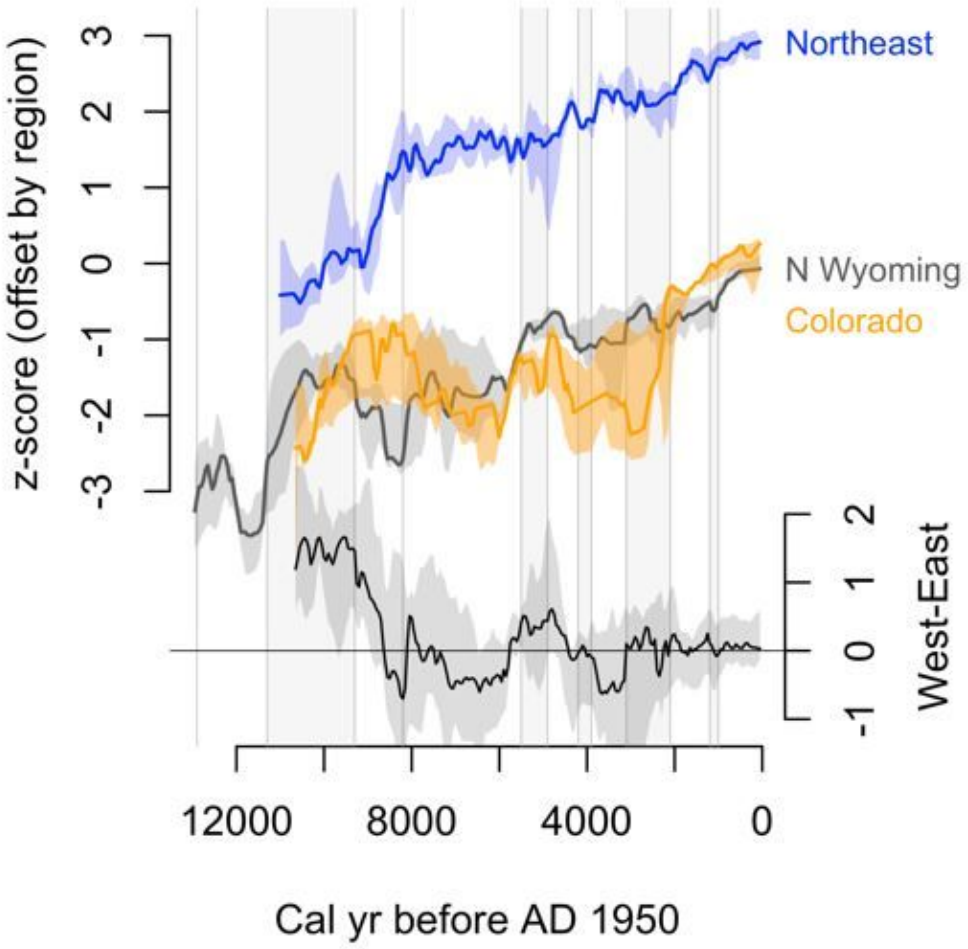

Figure 2

Averages of the reconstructions from the three regions: the Northeast (blue), northern Wyoming (black), and Colorado (orange). The difference between the Northeastern mean and the two western means (bottom) indicates the strength of the west-east precipitation gradient; the differences between Wyoming and Colorado highlight north-south variations in the west. The records are plotted as mean z-scores, offset for clarity. Gray bars are the same as in Fig. 1.

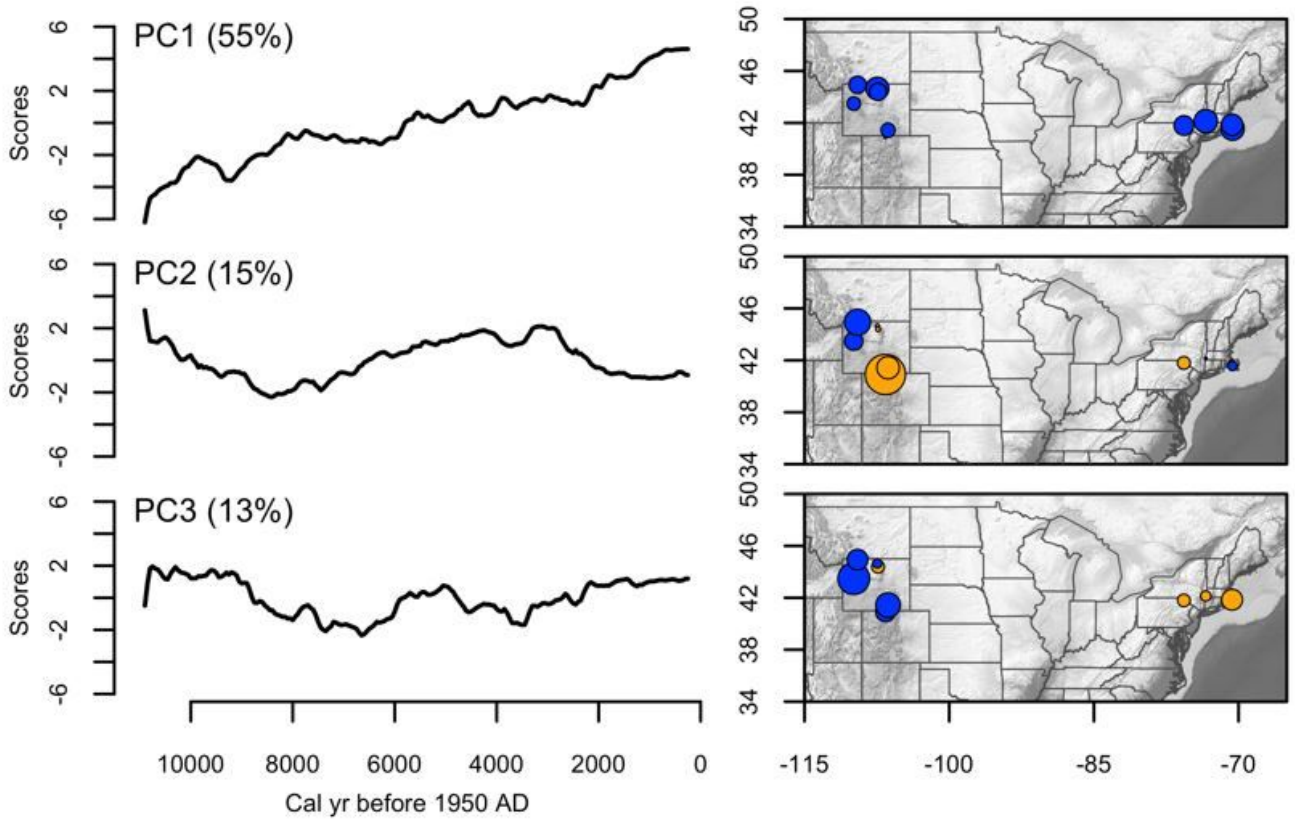

Figure 3

Plots of principal component scores and maps of the loadings for all records that span the full Holocene. Blue circles indicate positive loadings, orange negative loadings. Circle size relates to the magnitude of the loading. Loading magnitudes appear in Table 1.

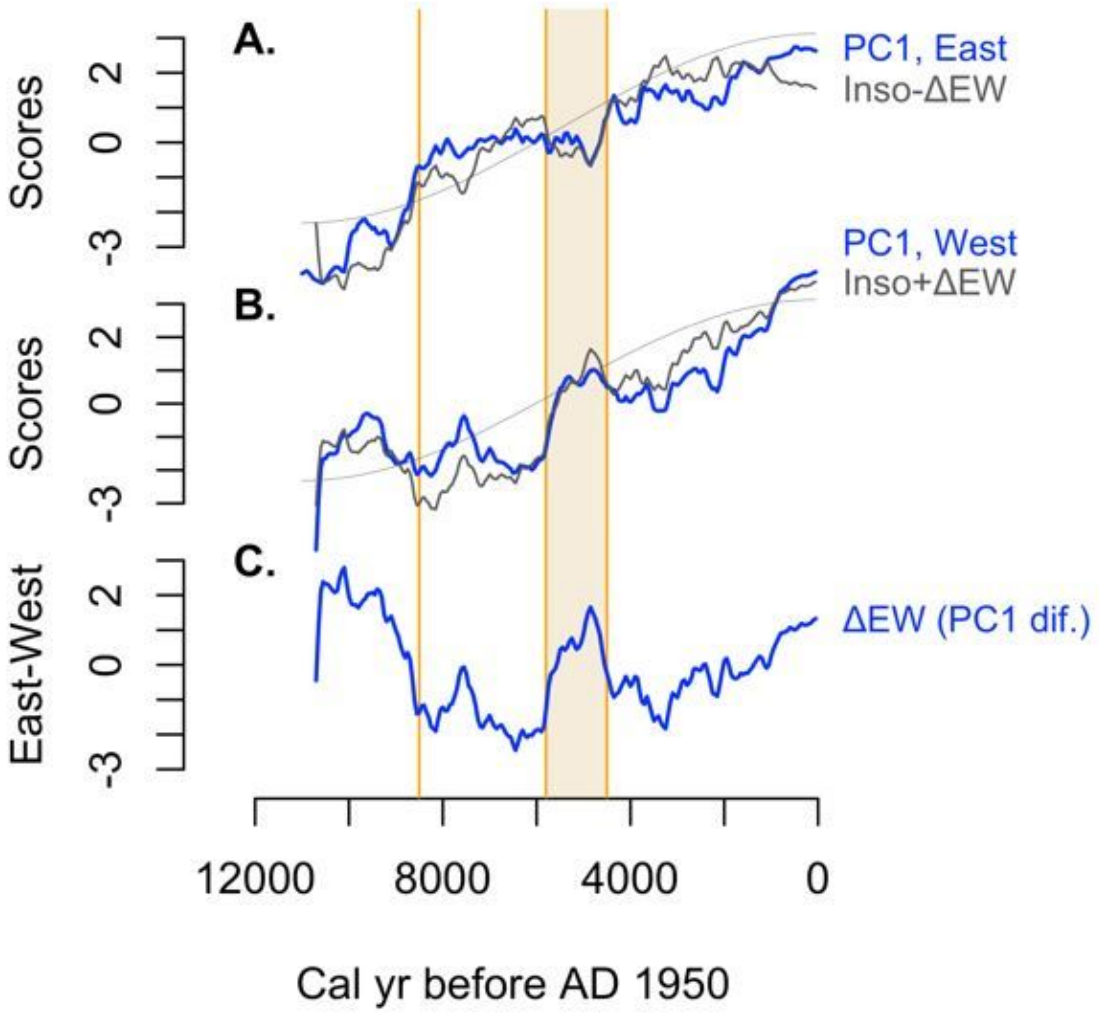

Figure 4

Plots of principal component scores for all records that span the full Holocene from A) eastern lakes and B) western lakes. C) △E-W represents the difference (dif.) between the two time-series of region PC1 scores in A and B. Bold gray lines indicate combinations of the △EW curve and a scaled precession curve ("Inso") represented by thin gray lines in A and B. Orange vertical lines mark major step changes at 8.5, 5.8, and 4.5 ka. Orange shading marks the anomalous millennium between the later two.

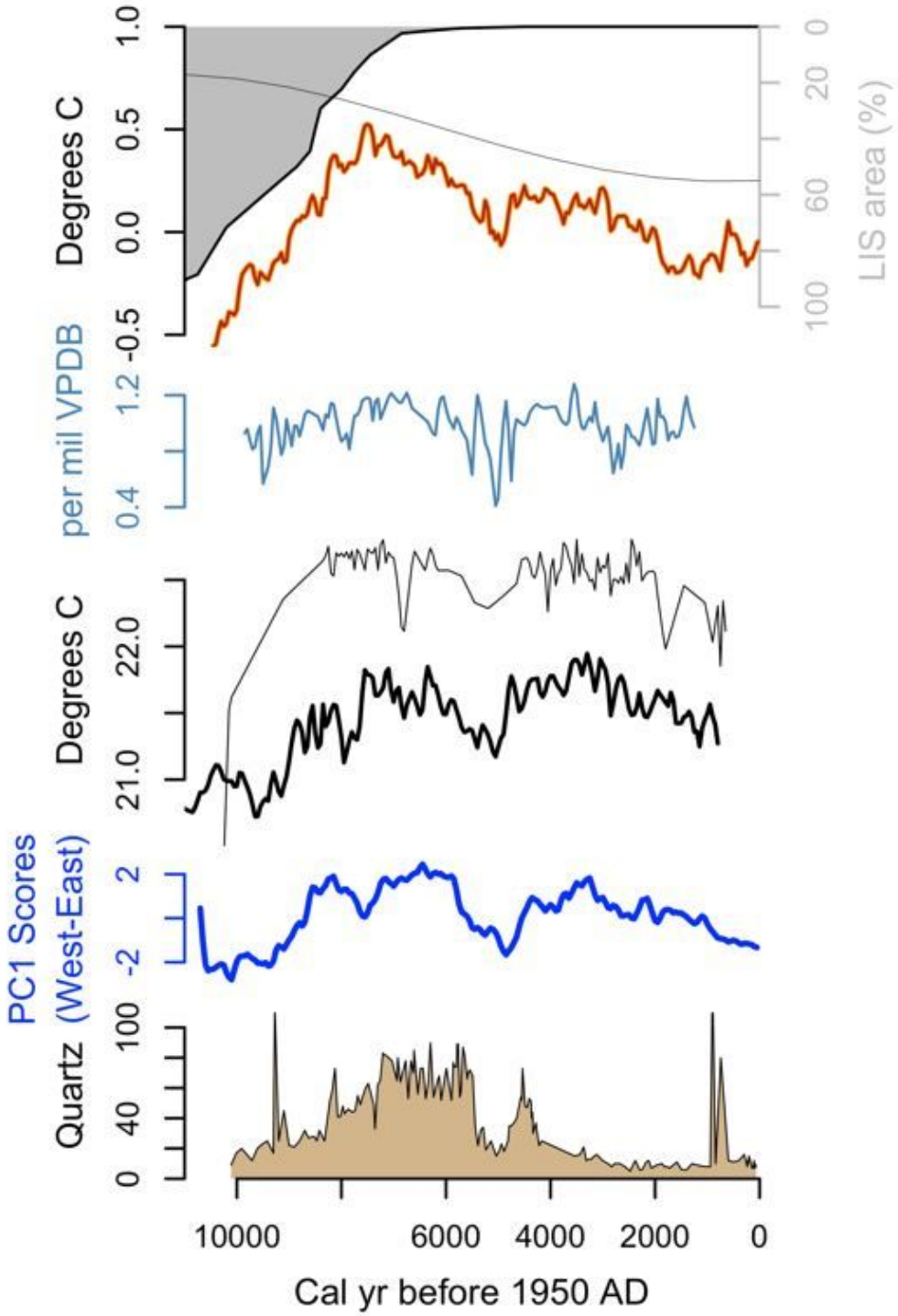

Figure 5

Time series of the area of the Laurentide ice sheet (filled gray)(Dyke 2004) and June insolation anomalies (gray line)(Berger and Loutre 1991) represent the long-term Holocene climate forcing trends, but other records including the difference between eastern and western lake-level records (regional PC1 score differences, the inverse of "△EW" from Fig. 4, bold blue line) record millennial variations, such as from 5.5-4.5 ka. Other series include carbon isotopes from the North Atlantic (thin blue line)(Oppo et al. 2003); mean temperatures of the warmest month from mid-latitude North America (as anomalies from the Holocene mean, orange line), mid-

continent North America (a 6-record mean, bold black line), and Sharkey Lake, Minnesota (thin black line) (Shuman and Marsicek 2016); and dust deposition at Elk Lake, Minnesota (tan filled)(Dean 1997).

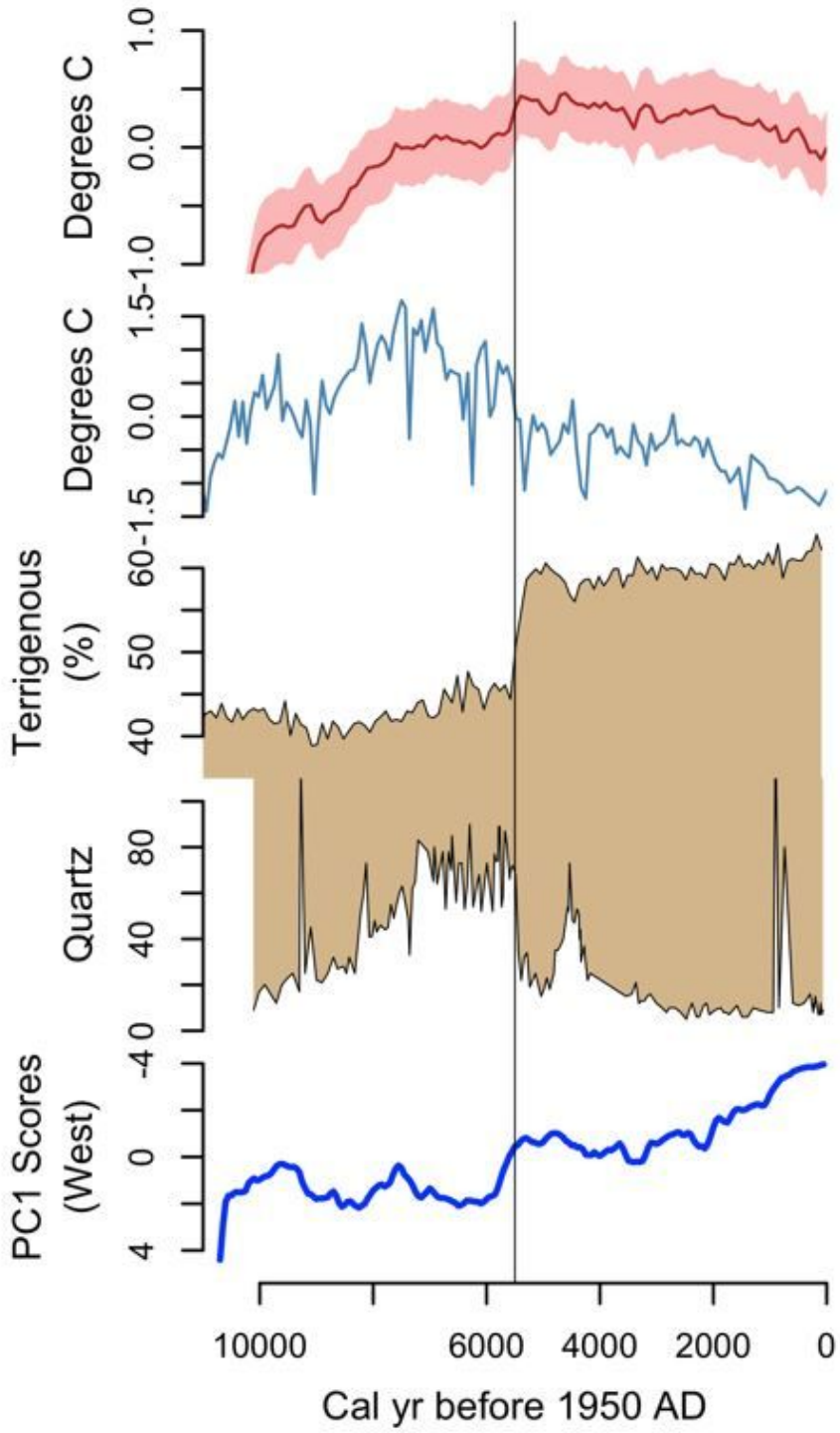

Figure 6

A mid-Holocene shift at 5.5 ka appears in the mean annual temperatures of Europe and North America (red) (Marsicek et al. 2018), detrended sea-surface temperatures from the Scotian Margin (thin blue line)(Sachs 2007), dust deposition from the west African margin of the Atlantic Ocean (top of tan shading)(deMenocal et al. 2000a) and Elk Lake, Minnesota (bottom of tan shading)(Dean 1997), and the PC1 scores from the western lakes from Fig. 4 (bold blue line, bottom).

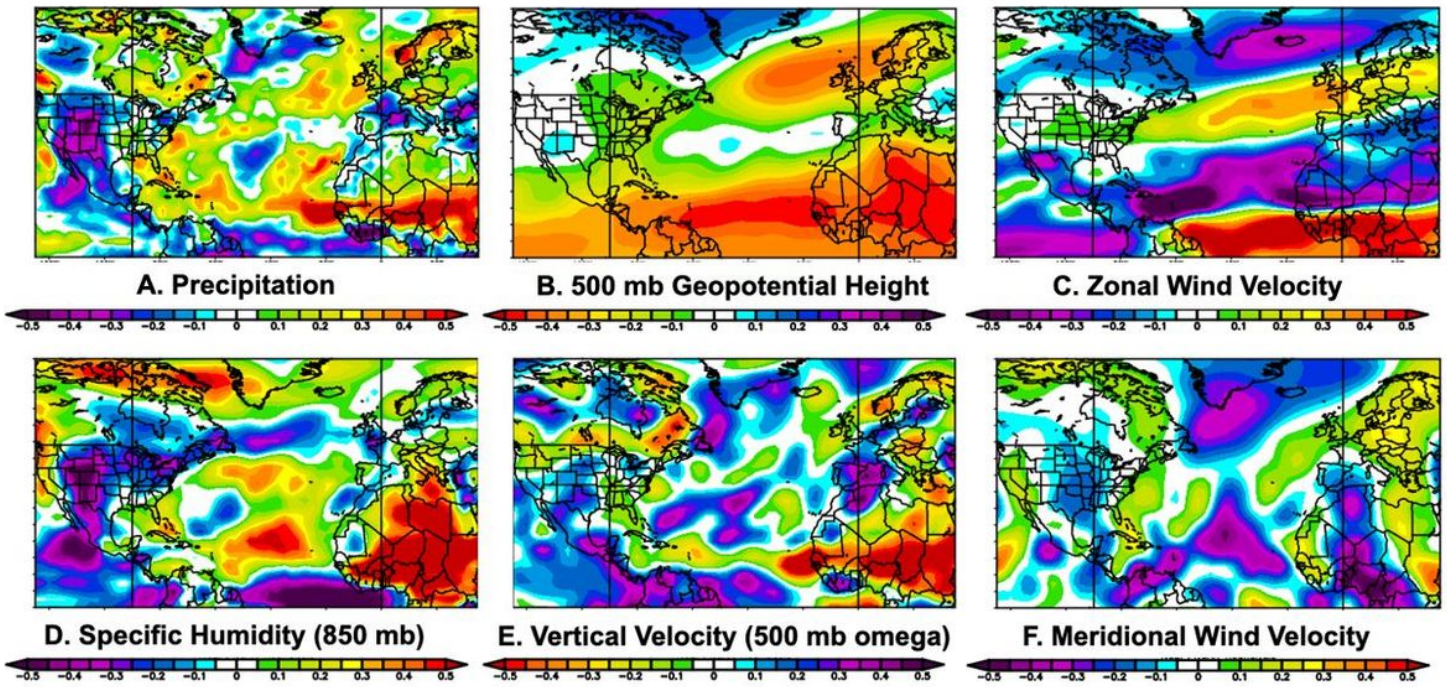

Figure 7

Correlations of June-August Sahel precipitation with precipitation, specific humidity at 850 mb height, geopotential height and zonal, meridional, and vertical velocities (omega) at 500 mb height from 1948-2015 in NCEP/NCAR Reanalysis (from www.psl.noaa.gov/data/correlation/). Blue colors indicate increased precipitation, increased geopotential heights, increased specific humidity, and increased velocities and uplift when Sahelian precipitation decreases; red colors indicate the opposite.

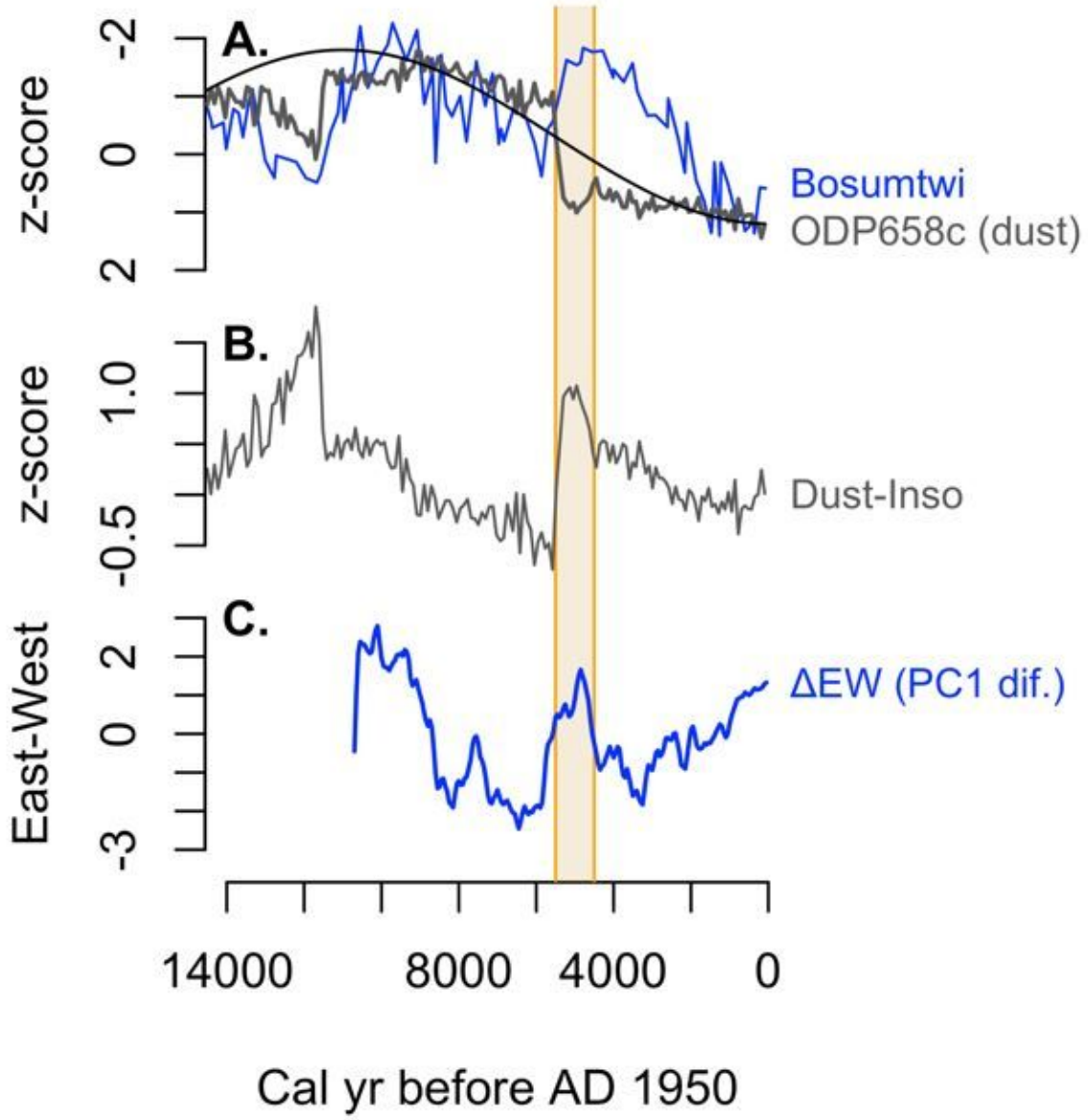

Figure 8

Comparison of the Lake Bosumtwi, Ghana, hydrogen isotope record (blue line, A)(Shanahan et al. 2015) and the ODP658c dust record from off west Africa (gray line, A)(deMenocal et al. 2000a) with precession ("Inso") trends (black line, A) and potential millennial variations indicated by B) subtracting the precession trend from the dust record and C) the difference in the first principal components ("PC1 dif.") from the eastern and western North American lakes as in Fig. 4C. The African records are plotted as z-scores and oriented to indicate wet as up, dry as down. Orange band marks the interval from 5.5-4.5 ka.